Polarization of emission in asymmetric rotors. I. The effects of elastic collisions, electron and nuclear spins

Kaspars Truhins, Zeyad T. Al Wahabi, Marcis Auzinsh,[a] Anthony J. McCaffery, and Zaid Rawi

School of Molecular Sciences, University of Sussex, Brighton BN1 9QJ, United Kingdom

We report measurements of the linear and circular polarization ratios as a function of rotational state for the asymmetric rotor NH_2. This molecule displays fine structure splitting from its unpaired electron and hyperfine structure from coupling with the nuclear spins. We present a theory of polarized emission for this molecule which includes the effects of fine and hyperfine interactions. These have a marked effect on the polarization ratios and are well described by a theory in which the effect of electron and nuclear spin are introduced as time-independent perturbation coefficients. We find that theory predicts different values of polarization ratio according to the manner of coupling of the proton nuclear spins. The best fits to experimental data are obtained when the coupling follows a physically intuitive scheme rather than that usually adopted. When all intramolecular couplings due to electron and nuclear spins are properly accounted for; *there is no depolarization that may be attributed to the effect of elastic collisions*. Thus, as in the case of diatomic molecules, orientation and alignment show a marked stability to change by collision. © *1997 American Institute of Physics.* [S0021-9606(97)00509-6]

I. INTRODUCTION

The observation of polarized fluorescence from excited molecules in the gas phase has a lengthy history[1] though only in recent years has this phenomenon been studied systematically and with rotational state resolution. With relatively few exceptions, these state resolved experiments have been carried out on diatomic molecules. The principal conclusion from this work is of stereodynamical significance and, in brief, is that reorientation of the *j*-vector by elastic collisions has low probability in diatomics[2–4] with cross sections typically two orders of magnitude lower that those for *j*-changing.[5] Recent reviews describe these experiments and their significance in terms of collision theories.[6,7]

This earlier work established that before polarized fluorescence data may be used to determine the extent of *collisional* depolarization, the effects of intramolecular interactions, particularly those involving angular momentum coupling, must be accounted for. One such is the nuclear hyperfine interaction, known to have a strong depolarizing effect particularly at low *j*-value. The degree of hyperfine depolarization is governed by the strength of coupling of nuclear spin to rotational angular momentum and on the lifetime of the molecular excited state. Theoretical treatments of fluorescence polarization in molecules representing two limiting coupling cases have been published. The first is the strong coupling regime,[8] characterized by long radiative lifetime and large hyperfine constant and the second, or weak coupling limit,[5] results when radiative lifetime is short and hyperfine constant small. Experimental results on molecules representing these two limiting cases[3,5] indicate that all depolarization effects may be accounted for in terms of the

intramolecular angular momentum couplings and there is no component of the depolarization that may be attributed to the effects of elastic collisions.

Here we describe an experimental and theoretical study of polarization of rotationally resolved fluorescence in a bent *triatomic* molecule possessing both nuclear and electron spin. The principal motivation for this study was the investigation of collisional reorientation in a system for which spectroscopic states are identifiable in terms of vectors in the molecule frame. This is of considerable significance in the study of dynamical stereochemistry. However the effects of intramolecular coupling of electron and nuclear spin with rotational angular momentum must be untangled before polarized fluorescence data may be interpreted in terms of collisional effects. This is particularly important for NH_2 since relatively low rotational states are accessed by laser excitation and these are likely to be most affected by fine and hyperfine interactions.

In addition, radicals possessing nuclear spin play an important role in, for example, atmospheric and combustion chemistry. An earlier treatment by Zare and co-workers[9] was in the context of alignment of diatomic radicals as products of photodissociation processes. The theory presented here is for the case of single quantum level preparation using linearly or circularly polarized radiation with state-resolved detection of polarized fluorescence. This development, which is for the resonance lines only, applies equally to diatomics as to asymmetric rotor molecules.

There have been many spectroscopic studies of NH_2 and, as a result, the constants for both ground and excited state are reasonably well established. Rotational state-resolved, linearly polarized fluorescence in this molecule was reported in 1975 by Kroll.[10] Spin doublets were not resolved and formulas presented for the polarization ratio neglected the nuclear

hyperfine interaction. Whitaker and McCaffery[11] reported circular polarization ratios for resonance and collisional transfer features in NH_2. The results were interpreted using a modified version of a treatment based on the Born approximation introduced by Dixon and Field.[12] This was only partially successful in interpreting the polarization of transfer features, emphasizing the unsuitability of an approximation based on the long-range potential in describing rotational transfer, which represents scattering from the repulsive wall.

This contribution reports linear and circular polarization measurements made on the resonance lines of a number of $N_{k_a k_c}$ states of NH_2 following polarized excitation of those states. Theoretical expressions are derived for the effect of electron and of nuclear spin on the polarization of resolved fluorescence. These predicted values are compared to experiment and found to give an excellent account when the nuclear spins are coupled in what could be thought of as a physically intuitive fashion rather than that conventionally adopted for spectroscopic purposes. The more complex theoretical problem of polarization of collisionally populated transfer features is treated in a separate publication.

II. THEORY

A. Excitation and detection in a state multipole basis

This section follows the density matrix treatment of Bain and McCaffery.[13] In expressions for polarization ratios of the resonance lines, the molecule-fixed projection quantum numbers k_a and k_c do not enter and therefore much of the theory developed for diatomic molecules may be carried over. Upon excitation the molecule undergoes a (rotationally resolved) electric dipole transition from the ground rovibronic state α'', N'' to the excited state α, N. Note that according to spectroscopic convention N represents rotational angular momentum for molecules that possess electron spin. In such a case $\mathbf{J}=\mathbf{N}+\mathbf{S}$. When molecules are excited using polarized radiation, the excited state density matrix elements are given by

$$^{NN}\rho_{M_1 M_2}(\hat{\epsilon}) \propto \sum_{M''} \langle \alpha N M_1 | \hat{\epsilon} \cdot \mathbf{d} | \alpha'' N'' M'' \rangle$$
$$\times \langle \alpha N M_2 | \hat{\epsilon} \cdot \mathbf{d} | \alpha'' N'' M'' \rangle^*, \qquad (1)$$

where $\hat{\epsilon}$ is the laser polarization vector, d is the electric dipole moment operator, and α, α'' represent all molecular quantum numbers other than those involving molecular rotation.

In the case of circularly polarized excitation the quantization axis is along the laser propagation direction, denoted $\hat{O}$, then the dipole transition can be described in spherical coordinates by[14]

$$\hat{\epsilon} \cdot \mathbf{d} = (-1)^{q_A} \epsilon^1_{q_A} \cdot d^1_{-q_A}, \qquad (2)$$

where $q_A = +1$ for left circularly polarized light and $q_A = -1$ for right circularly polarized light.

For linearly polarized excitation the quantization axis is along the laser polarization direction, denoted $\hat{z}$ and the dipole transition is

$$\hat{\epsilon}_z \cdot \mathbf{d}_z = \epsilon^1_0 \cdot d^1_0. \qquad (3)$$

We utilize the state multipole formalism in which the excited state M distribution is represented by irreducible components of the density matrix

$$^{NN}\rho_Q^K = \sum_{M_1 M_2} (-1)^{N-M_1} (2K+1)^{1/2}$$
$$\times \begin{pmatrix} N & N & K \\ M_1 & -M_2 & -Q \end{pmatrix}\ ^{NN}\rho_{M_1 M_2}, \qquad (4)$$

K is the tensor rank which, for the case of a weak incident radiation field is limited to the values 0, 1, and 2.

The expression appropriate to circularly polarized excitation is obtained through application of the Wigner–Eckart theorem,[15] which in general form may be stated as

$$\langle \alpha' j' m' | T_Q^K | \alpha j m \rangle = (-1)^{j'-m'} \begin{pmatrix} j' & K & j \\ -m' & Q & m \end{pmatrix}$$
$$\times \langle \alpha' j' \| T^K \| \alpha j \rangle, \qquad (5)$$

where T_Q^K is a tensor operator of rank K and component Q.

The state multipoles formed in the upper state following circularly polarized excitation then become

$$^{NN}\rho_0^K(q_A, \hat{O}) \propto \sum_{M_1 M''} (-1)^{N-M} (2K+1)^{1/2}$$
$$\times |\langle \alpha N \| d^1 \| \alpha'' N'' \rangle|^2 \begin{pmatrix} N & N & K \\ M_1 & -M_2 & 0 \end{pmatrix}$$
$$\times \begin{pmatrix} N & 1 & N'' \\ -M & q_A & M'' \end{pmatrix}^2. \qquad (6)$$

The 3-j symbols in Eq. (8) may be rearranged into one 6-j and one 3-j to eliminate the sums over M. The expression then becomes[13]

$$^{NN}\rho_0^K(q_A, \hat{O}) \propto (-1)^{N+N''+K+q_A} (2K+1)^{1/2}$$
$$\times \begin{pmatrix} 1 & 1 & K \\ q_A & -q_A & 0 \end{pmatrix} \begin{Bmatrix} 1 & 1 & K \\ N & N & N'' \end{Bmatrix}$$
$$\times |\langle \alpha N \| d_1^1 \| \alpha'' N'' \rangle|^2, \qquad (7)$$

where $q_A = \pm 1$.

For linearly polarized excitation the quantization axis is along the direction of the electric vector. $q_A = 0$ and the state multipole of the excited state is[13]

$$^{NN}\rho_0^K(\hat{z}) \propto \sum_{M, M''} (-1)^{N-M} (2K+1)^{1/2} |\langle \alpha N \| d^1 \| \alpha'' N'' \rangle|^2$$
$$\times \begin{pmatrix} N & N & K \\ M & -M & 0 \end{pmatrix} \begin{pmatrix} N & 1 & N'' \\ -M & 0 & M'' \end{pmatrix}^2 \qquad (8)$$

which on rearranging the 3-j symbols becomes

$$^{NN}\rho_0^K(q_A,\hat{z}) \propto (-1)^{N+N''+K}(2K+1)^{1/2}\begin{pmatrix} 1 & 1 & K \\ 0 & 0 & 0 \end{pmatrix}$$

$$\times \begin{Bmatrix} 1 & 1 & K \\ N & N & N'' \end{Bmatrix} |\langle \alpha N \| d_0^1 \| \alpha'' N'' \rangle|^2. \tag{9}$$

Equations (7) and (9) in conjunction with the known tensor rank of the electric dipole operator and properties of the 3-*j* symbols provide proof that multipoles of rank $K=0$, 1, and 2 and component $Q=0$ only are allowed.

Once formed, the polarized arrays of excited molecules evolve in time until either they suffer inelastic collision or undergo spontaneous dipole transitions to final state $\alpha''' N'''$. The intensity of fluorescence is given by

$$I \propto \sum_{M_1 M_2} {}^{NN}\rho_{M_1 M_2}(q_A) \cdot D_{M_1 M_2}(q_E), \tag{10}$$

where $D_{M_1 M_2}(q_E)$ is a detection matrix for the dipole transition from the state having projection quantum number distribution M_1 and M_2, and transition having emission polarization q_E. The detection matrix for the transition from rotational level N of the excited state to the final state N''' is

$$D_{M_1 M_2} = \sum_{M'''} \langle \alpha N M_1 | \hat{\boldsymbol{\epsilon}}_E \cdot \mathbf{d}_E | \alpha''' N''' M''' \rangle$$

$$\times \langle \alpha N M_2 | \hat{\boldsymbol{\epsilon}}_E \cdot \mathbf{d}_E | \alpha''' N''' M''' \rangle^*. \tag{11}$$

For circularly polarized excitation and detection the quantization axis is along the laser propagation direction thus $q_E = -q_A$ for I_- and $q_E = q_A$ for I_+. The intensity of polarized emission is given by

$$I_{q_E}^{q_A} \propto \sum_{KMM'''} {}^{NN}\rho^K(-1)^{N-M_1}(2K+1)^{1/2}$$

$$\times \begin{pmatrix} N & N & K \\ M & -M & -0 \end{pmatrix}$$

$$\times |\langle \alpha N M | \hat{\boldsymbol{\epsilon}}_E \cdot \underline{d}_E | \alpha''' N''' M''' \rangle|^2. \tag{12}$$

Using the Wigner–Eckart theorem and rearranging the 3-*j* symbols as before, the intensity of circularly polarized emission following circularly polarized excitation is

$$I_{q_E}^{q_A} \propto \sum_K {}^{NN}\rho^K(q_A)(-1)^{N+N'''+K+q_E}(2K+1)^{1/2}$$

$$\times \begin{pmatrix} 1 & 1 & K \\ q_E & -q_E & 0 \end{pmatrix} \begin{Bmatrix} 1 & 1 & K \\ N & N & N''' \end{Bmatrix}$$

$$\times |\langle \alpha''' N''' \| d_1^1 \| \alpha N \rangle|^2. \tag{13}$$

For linearly polarized excitation and detection the axis of quantization remains that for excitation (i.e., the electric vector direction) and $q_E = 0$. The detection matrix has the same form as for circular polarization Eq. (13). The intensity of emitted radiation of polarization parallel to that of the excitation radiation is

$$I_\parallel \propto \sum_{KMM'''} {}^{NN}\rho^K(-1)^{N-M}(2K+1)^{1/2}\begin{pmatrix} N & N & K \\ M & -M & 0 \end{pmatrix}$$

$$\times |\langle \alpha N M | \hat{\underline{\epsilon}}_{zE} \cdot \underline{d}_E | \alpha''' N''' M''' \rangle|^2 \tag{14}$$

which simplifies to

$$I_\parallel \propto \sum_K {}^{NN}\rho^K(-1)^{N+N'''+K}(2K+1)^{1/2}\begin{pmatrix} 1 & 1 & K \\ 0 & 0 & 0 \end{pmatrix}$$

$$\times \begin{Bmatrix} 1 & 1 & K \\ N & N & N''' \end{Bmatrix} |\langle \alpha''' N''' \| d^1 \| \alpha N \rangle|^2. \tag{15}$$

The perpendicular component of fluorescence intensity $I_\perp$ may be obtained by carrying out the rotation $R(0,\theta,0)$ on the detection polarization tensor.[15] As discussed above, only $Q=0$ components of the tensors are created in the excited state and hence only $Q=0$ terms can appear in the expression for the fluorescence polarization. The rotation is therefore $D_{00}^K(0,\theta,0)=P_K(\cos\theta)$, where $P_K(\cos\theta)$ is an associated Legendre function and $\theta=90°$. The intensity of fluorescence having perpendicular polarization component is then given by

$$I_\perp \propto \sum_K {}^{NN}\rho^K(-1)^{N+N'''+K}(2K+1)^{1/2}\begin{pmatrix} 1 & 1 & K \\ 0 & 0 & 0 \end{pmatrix}$$

$$\times \begin{Bmatrix} 1 & 1 & K \\ N & N & N''' \end{Bmatrix} P_K(0)|\langle \alpha''' N''' \| d^1 \| \alpha N \rangle|^2. \tag{16}$$

B. Hyperfine and fine depolarization

For molecules comprised of atoms possessing nuclear spin, the effects of the hyperfine interaction must be considered. This is known to depolarize rotationally resolved fluorescence in diatomic molecules particularly for those in low rotational states.[2,5] Two limiting cases were identified, the first or strong coupling case being found in diatomics (such as I_2) with relatively long lifetime and strong hyperfine coupling. In this case the slowly-precessing nuclear spin vector has time to couple fully to the rotational angular momentum during the excited state lifetime. In the weak coupling limit (Li_2 for example) the lifetime is short and coupling weak. Only a limited degree of vector coupling takes place during the excited lifetime and depolarizing effects are seen only in the lowest rotational states,[5] in contrast to the strong coupling regime in which effects can be discerned up to quite high rotational states.[3]

The ^2A state of NH_2 is in the first of these categories with hyperfine splittings of the order of 100 MHz (Ref. 16), and excited state lifetime of 10 μs.[17] In these circumstances the coupling of nuclear spin with the rotational angular momentum may be described using a formalism introduced by Blum[19] in which time independent perturbation coefficients are used to quantify the interaction

$$^{NN}G_I^K = \sum_F \frac{(2F+1)^2}{2I+1}\begin{Bmatrix} J & F & I \\ F & J & K \end{Bmatrix}^2. \tag{17}$$

In Eq. (20), $\mathbf{J}$ is the rotational angular momentum, $\mathbf{I}$ is the nuclear spin, and $\mathbf{F}$ is the total angular momentum, i.e.,
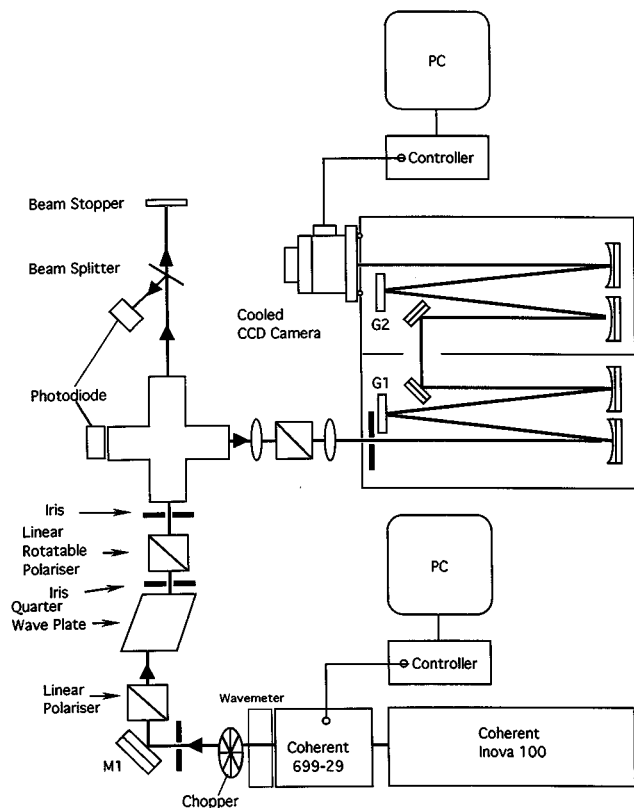
FIG. 1. Overview of experiment.

$$\mathbf{F} = \mathbf{J} + \mathbf{I}.$$

The fine splitting, which arises from the coupling of electron spin, S with the rotational angular momentum N can be treated using a similar expression, the perturbation coefficient in this case being given by[19]

$$^{NN}G_S^K = \sum_J \frac{(2J+1)^2}{2S+1} \begin{Bmatrix} N & J & S \\ J & N & K \end{Bmatrix}^2,$$ (18)

$$\mathbf{J} = \mathbf{N} + \mathbf{I}.$$

When both nuclear and electron spins need to be considered, the overall perturbation coefficient is obtained by combining the two coefficients given above in Eqs. (17) and (18)

$$^{NN}G^K = \sum_{J,F} \frac{(2J+1)^2(2F+1)^2}{(2S+1)(2I+1)} \begin{Bmatrix} N & J & S \\ J & N & K \end{Bmatrix}^2 \begin{Bmatrix} J & F & I \\ F & J & K \end{Bmatrix}^2.$$ (19)

Note this approach assumes that fine and hyperfine splittings are spectrally unresolved (or components summed when there is partial or complete resolution).

The physical picture that the perturbation coefficients represent is one in which the rotational angular momentum and the nuclear and electron spin vectors are uncoupled during the excitation process. Once the excited state is formed these vectors recouple. The perturbation coefficients of Eq. (19) represent the probability that in the excited state rota-

tional angular momentum N will couple with the electron spin S to form J and that J will couple with the total nuclear spin I to form total angular momentum F.

The general form of the expression for intensity of emission of a specified polarization q_E following excitation by light of polarization q_A in the presence of these additional angular momentum couplings can be written as

$$I_{q_E}^{q_A} = \sum_{K,Q} {}^{JJ}\rho_Q^K(q_A) \cdot {}^{JJ}G_Q^K \cdot {}^{JJ}D^K(q_E) \cdot P_K(\cos\theta).$$ (20)

In this equation, $P_K(\cos\theta)$ is an associated Legendre function and θ is the angle between excitation and detection directions in the case of circularly polarized excitation, or the angle between excitation and detection polarization vectors for linearly polarized excitation. The final expression for rotationally resolved polarized fluorescence intensity in molecules in which there is nuclear and electron spin coupling to the rotational AM is the following:

$$I_{q_E}^{q_A} \propto \sum_K \sum_F \sum_J \frac{(2J+1)^2(2F+1)^2(2K+1)}{(2S+1)(2I+1)}$$

$$\times \begin{pmatrix} 1 & 1 & K \\ q_A & -q_A & 0 \end{pmatrix} \begin{pmatrix} 1 & 1 & K \\ q_E & -q_E & 0 \end{pmatrix} \begin{Bmatrix} 1 & 1 & K \\ N & N & N'' \end{Bmatrix}$$

$$\times \begin{Bmatrix} 1 & 1 & K \\ N & N & N''' \end{Bmatrix}$$

$$\times \begin{Bmatrix} N & J & S \\ J & N & K \end{Bmatrix}^2 \begin{Bmatrix} J & F & I \\ F & J & K \end{Bmatrix}^2 P_K(\cos\theta),$$ (21)

III. EXPERIMENT

Recent publications describe the flow-reactor system used to create NH_2 radicals from hydrazine using H atoms generated by microwave discharge of H_2.[18] Under these experimental conditions the principal collision partner is known to be H atoms.[12] The present experiment differs from that reported earlier in two significant respects. Here we have measured emission spectra of groups of lines using a CCD array in conjunction with a double grating monochromator. The CCD has extremely precise timing. This enabled parallel and perpendicular-polarized emission spectra to be measured by manual rotation of the laser polarization, setting the collection time to be identical for both measurements.

Sets of integrated line intensities were manipulated using the CCD software to produce values of parameter P. Small changes in the intensity of laser radiation on rotating the polarization through 90° were measured using a modulation method with detection by a photodiode linked to a lock-in amplifier. This gave a correction factor which was applied to the CCD intensities. Depolarization by cell windows was also measured directly and a small correction ($\sim$1%) was found necessary for this effect. Great care was taken to exclude all stray laser radiation in this, effectively unmodulated, experiment. There are substantial gains in accuracy and sensitivity in the method employed due to the high duty factor inherent in the technique.
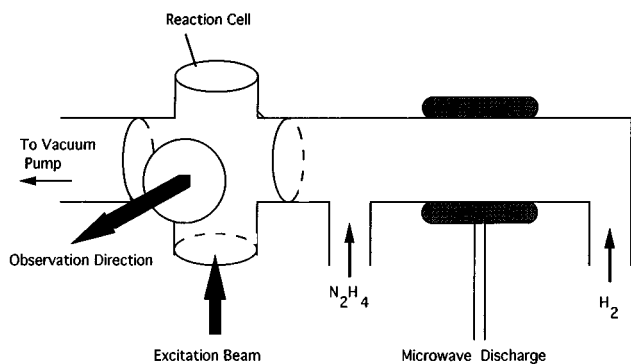
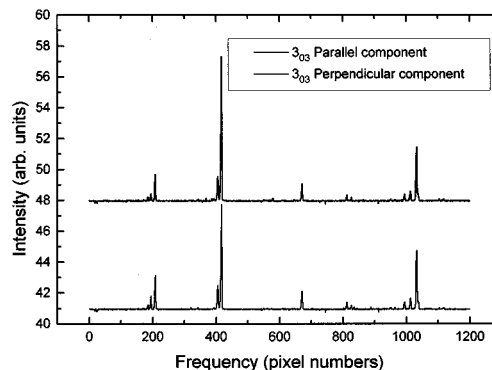FIG. 2. Detail of optical arrangement for observation of fluorescence polarization.

FIG. 3. Polarized fluorescence data as recorded by the CCD. This yields $I_\parallel$ and $I_\perp$ which are then added and subtracted to obtain polarization ratios.

The second principal difference lies in the collision environment employed here compared to those of Ref. 18. In this work, gas pressures of around 2.5×10^{-1} Torr were typically used, an order of magnitude lower than in previous work. This ensures formal single collision conditions. Note however that earlier studies had demonstrated using extensive pressure dependence, that even at considerably higher cell pressures, the transfer data were the result of single collision events. The earlier work established that the earth's magnetic field had no significant influence on the polarization measurements[18] through the use of Helmholtz coils to create a zero field environment. Figures 1 and 2 display overview and detail of the experiment, respectively.

The microwave discharge power utilized throughout this experiment was 60 W and H atoms were generated approximately 60 cm upstream of the reaction zone. Molecular hydrogen and hydrazine enter the reaction region separately carried by He gas and controlled by needle valves. The reaction chamber has optical ports through which optical access is available perpendicular to the direction of flow. The discharge tube and flow line were etched with 50% hydrofluoric acid prior to each experiment in order to reduce radical destruction at the walls. The output from an argon-pumped ring dye laser (Coherent 699.29) was directed to cross the flow some 10 cm from the hydrazine inlet. The spectral width of the laser is 1 MHz or less and thus is considerably narrower than the Doppler width of the $X\,^2B_1 - A\,^2A_1$ transition, measured, by scanning across the line profile, to be around 800 MHz. This measurement also permitted an accurate estimate of the temperature of $^2A_1\mathrm{NH}_2$ in the center of the reaction zone to be made which was found to be 346 ± 13 K.

NH_2 was excited from $X\,^2B_1$ to rotational levels of the (0,9,0) vibrational manifold of its first excited electronic state ($A\,^2A_1$). The presence of the unpaired electron causes each level to split into two; the upper spin doublet $J = N + \frac{1}{2}$ and the lower spin doublet $J = N - \frac{1}{2}$. Nitrogen has nuclear spin $I_N = 1$ and for hydrogen $I_H = \frac{1}{2}$. The hyperfine splitting was not resolved in this Doppler-limited experiment nor in most cases was the fine structure splitting. Accessible rotation levels were $N = 1$–7. This molecule obeys c-type selection rules and hence the transition dipole moment is in the

direction of c molecular axis. Line positions were found to be in good agreement with the published tables of Dressler and Ramsay.[20]

Fluorescence from the excited radicals was focused into a Spex double monochromator and the dispersed light detected using a CCD camera. For each transition two sets of data were obtained, first, when the polarization of the excitation beam was parallel to that of the fluorescence and second, when perpendicular. The beam intensity after the cell was measured using a lock-in amplifier so as to correct the experimental data for changes in laser intensity. The total fluorescence from the cell was also monitored throughout the experiment to ensure chemical conditions in the reaction cell remained constant throughout the experiment. The resulting CCD images were computer-manipulated to produce a final spectrum of intensity difference and intensity sum (and hence the polarization ratio for each resolved transition) vs wavelength. Figure 3 shows an example of data recorded in this fashion.

The linear and circular polarization ratios, P and C, respectively, are defined in the conventional way

$$P = \frac{I_\parallel - I_\perp}{I_\parallel + I_\perp}, \tag{22}$$

where $I_\parallel$ and $I_\perp$ are the intensities of fluorescence having polarization parallel with or perpendicular to the electric vector of the exciting radiation, respectively,

$$C = \frac{I_+ - I_-}{I_+ + I_-}, \tag{23}$$

where I_+ and I_- are the intensities of the emitted radiation having polarization in the same $(+)$ or opposite $(-)$ sense to that of the excitation radiation.

The techniques used for measuring circular polarization ratios are described in Ref. 18. C values may only be measured in $0°$ or $180°$ geometries and so the experimental configuration was changed from that used for the measurement of P. Linearly polarized laser radiation was circularly polarized by means of a Fresnel rhomb. The circular polarization of emission was determined using a photoelastic modulator locked to a synchronous photon counter. In this experiment

the monochromator was scanned to produce individual spectral lines for which intensity and polarization were recorded simultaneously.

IV. RESULTS

To compare theory with experiment the assumption was made that upper and lower state spin doublets were not resolved in the experimental data. This is a good approximation for the excitation process since although the laser linewidth is narrow compared to spin splitting, the latter is less than the Doppler width of the Σ-states studied here. The hyperfine components will all be Doppler shifted into resonance with the exciting light though will not be equally populated due to having different Hönl–London factors. As discussed above, coherence effects can be neglected and the time independent perturbation coefficients of Eq. (19) provide a satisfactory basis for the calculation.

In calculating P and C, hyperfine interactions from the N nucleus and the two H nuclei must be included. The ^{14}N splitting is expected to be the larger of these and to couple most strongly with the rotational angular momentum. Previous treatments of the coupling of the two protons in this molecule[22] have assumed their spins to be coupled to one another *prior* to their interaction with the combined rotational and ^{14}N angular momentum. For the initial calculations this $JI_NF_NI_{H_2}F$ coupling scheme was used in calculations of intensity (21) and polarization (22) and (23). In this scheme $I_{H_2} = 1,0$ in analogy to the hydrogen *molecule*, giving rise to the identification of levels of NH_2 as ortho states or para-states, respectively.

This coupling scheme however resulted in unsatisfactory agreement with experimental data. Particularly disjoint is the predicted alternation in polarization ratios for odd and even N values which is not seen experimentally. We therefore tested an alternative, more physically reasonable coupling scheme namely $JI_NF'I_HF''I_HF$ coupling, where $I_H=1/2$ the hydrogen *atom* nuclear spin. This corresponds to Hund's case $b_{\beta J}$ coupling.[21] The expression for intensity then becomes

$$I_{q_B}^{q_A} \propto \sum_K \sum_{F'F''F} \sum_J \sum_S \frac{(2J+1)^2(2F'+1)^2(2F''+1)^2(2F+1)^2(2K+1)}{(2S+1)(2I_H+1)^2(2I_N+1)} \begin{pmatrix} 1 & 1 & K \\ q_A & -q_A & 0 \end{pmatrix} \begin{pmatrix} 1 & 1 & K \\ q_E & -q_E & 0 \end{pmatrix} \begin{Bmatrix} 1 & 1 & K \\ N & N & N'' \end{Bmatrix}$$

$$\times \begin{Bmatrix} 1 & 1 & K \\ N & N & N''' \end{Bmatrix} \begin{Bmatrix} N & J & S \\ J & N & K \end{Bmatrix}^2 \begin{Bmatrix} J & F' & I_N \\ F' & J & K \end{Bmatrix}^2 \begin{Bmatrix} F' & F'' & I_H \\ F'' & F' & K \end{Bmatrix}^2 \begin{Bmatrix} F'' & F & I_H \\ F & F'' & K \end{Bmatrix}^2 P_K(\cos\theta). \quad (24)$$

The results of all calculations are presented in Tables I–III and are displayed as plots of C or P vs N in Figs. 4, 5, and 6 together with the experimental points. Results from three sets of calculations are shown. In increasing ability to match experiment these are as follows. First are data points calculated using the formulas for C and P with no additional angular momentum coupling, i.e., no fine or hyperfine interactions. These formulas are the well known forms found in standard sources, e.g., the texts of Feofilov[1] and Zare.[15] The second set utilizes the formulas derived above with fine and hyperfine interaction included. However, they use the form of proton hyperfine coupling that is referred to above as H_2 molecule coupling. Thus the proton spins are first coupled together and then coupled to the combined ^{14}N-rotation an-

gular momentum. The third set of calculations use the more intuitive form of coupling suggested above in which the proton nuclear spins are coupled *separately* to the combined ^{14}N-rotation angular momentum. This form of coupling is expected to provide a better physical representation of the actual interactions within the molecule, given the separation of the two protons by the central N atom.

Two sets of experimental linear polarization ratios and one of circular polarization ratios are shown in Figs. 4–6 all plotted as a function of N. Figure 4 shows C values for a set of QP transitions and Figs. 5 and 6 are for sets of QQ and

TABLE I. The CPR experimental and theoretical values for NH_2.

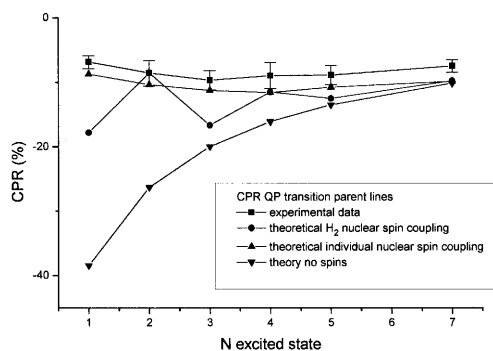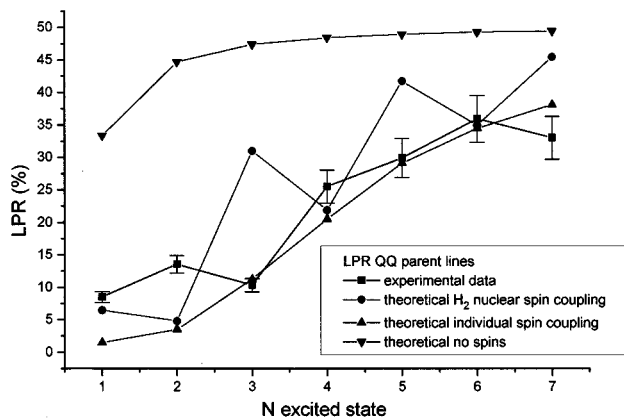| | Circular polarization ratios $Q\uparrow P\downarrow$ | | | |
N	C_{exp}	$C_{theor.\ no\ spins}$	$C_{theor.J+I_N+I_H+I_H}$	$C_{theor.J+I_N+I_{H_2}}$
1	−6.88	−38.46	−8.77	−17.81
2	−8.60	−26.32	−10.38	−8.55
3	−9.70	−20.00	−11.28	−16.68
4	−9.00	−16.13	−11.60	−11.52
5	−8.90	−13.51	−10.81	−12.53
7	−7.50	−10.20	−9.87	−9.79

FIG. 4. Circular polarization ratios for QP resonance lines plotted as a function of excited state N value.

TABLE II. The LPR experimental and theoretical values for NH_2.

	Linear polarization ratios $Q\uparrow Q\downarrow$			
N	P_{exp}	$P_{theor.\ no\ spins}$	$P_{theor. J+I_N+I_H+I_H}$	$P_{theor. J+I_N+I_{H_2}}$
1	8.49	33.33	1.44	6.45
2	13.53	44.68	3.51	4.78
3	10.30	47.37	11.22	30.99
4	25.51	48.42	20.49	21.88
5	29.92	48.95	29.09	41.72
6	35.93	49.25	34.48	34.92
7	33.00	49.44	38.09	45.46

TABLE III. The LPR experimental and theoretical values for NH_2.

	Linear polarization ratios $Q\uparrow R\downarrow$			
N	P_{exp}	$P_{theor.\ no\ spins}$	$P_{theor. J+I_N+I_H+I_H}$	$P_{theor. J+I_N+I_{H_2}}$
2	−14.46	−63.64	−3.59	−4.94
3	−18.75	−52.94	−9.62	−30.46
4	−26.60	−47.83	−16.99	−17.86
5	−19.84	−44.83	−23.14	−36.20
6	−31.28	−42.86	−27.02	−27.45
7	−22.08	−41.46	−29.49	−37.04

QR transitions, respectively. The profound effect of nuclear and electron spin on the polarization ratio can be seen very clearly on comparison of all data sets with the prediction of the ''rotation-only'' calculation. In both calculations the depolarizing effect of intramolecular angular momentum coupling is seen to decrease as N increases and by $N=7$ the values have begun to converge.
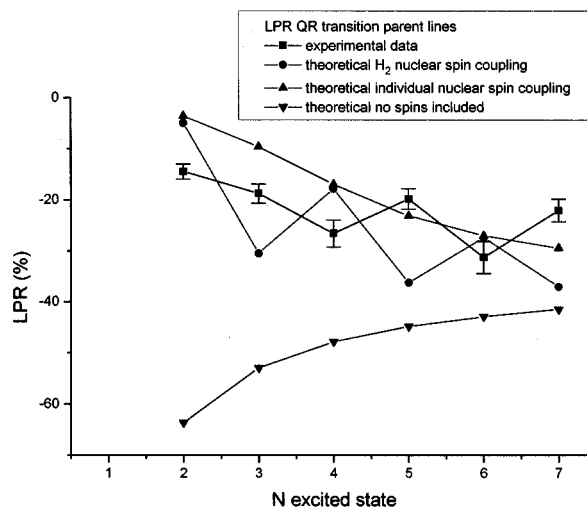
The results of calculations based on the two different proton spin coupling cases are intriguing. The coupled proton spin (molecular H_2) model predicts marked alternations for odd and even N values (the ortho and para levels, respectively). These alternations are generally not seen in the data although the calculated para level polarization ratios are generally closer to experiment than are the ortho levels. On the other hand the agreement between calculated values and experiment is particularly good for the more physically appealing ''separately coupled H-atom'' scheme. Although the data points are not always within experimental error bars, the overall shape of the P or C vs N curves gives closest agreement in this latter coupling case with many points lying within experimental uncertainty. The closeness of the experimental results to those predicted with no contribution from collisional interactions implies that, as was found in the case of diatomic molecules,[6,7] *there is little reorientation of the rotational angular momentum vector that can be attributed to the effects of elastic collisions.*

V. CONCLUSIONS

This study set out to determine the effect of elastic collisions on the orientation of the rotational angular momentum vector in the triatomic molecule NH_2. In order to assess the effect of collisions it was necessary to account for the depolarizing effects of electron and nuclear spin. As can be seen from the results, these are very marked and an interpretation based on comparison of the data with a calculation that ignores fine and hyperfine effects would be very misleading. Furthermore the manner in which hyperfine interactions, particularly those of the protons, are coupled has a surprisingly large influence. The most satisfactory results are obtained from the calculation when the most intuitively appealing coupling scheme, that of separate proton coupling, is adopted. This is contrary to spectroscopic convention in these triatomic hydrides. However, it is probably premature to suggest that the scheme we have used should be more widely adopted. What little data exist in which the hyperfine levels have been resolved indicates that the hyperfine interaction varies very markedly from ground to excited states and also with vibrational level accessed.[22] The rotational levels studied here are in the (0,9,0) vibrational manifold and

FIG. 5. Linear polarization ratios for QQ resonance lines plotted as a function of excited state N value.

FIG. 6. Linear polarization ratios for QR resonance lines plotted as a function of excited state N value.

hence many quanta of the bend vibration are excited. The influence of the bend vibration on the hyperfine interaction needs further study.

The object of this work, as stated above, was to examine the stability of the state multipoles of orientation and alignment to elastic collisions. It is clear that $K=1, 2$ are changed only slowly by collision, as with diatomic molecules. This work is a necessary prelude to a study of change of orientation and of alignment as a result of *inelastic* collisions which we shall report shortly. It is of interest to note that the molecular frame projection quantum numbers k_a and k_c disappear in the expressions for resonance line polarization ratios but are an essential element in the transfer features. Since these quantum numbers allow direct access of molecular coordinates from the laboratory frame, valuable stereodynamical information may be anticipated.

ACKNOWLEDGMENTS

[1] P. P. Feofilov, *The Physical Basis of Polarized Emission* (Consultants Bureau, New York, 1961).

[2] R. Clark and A. J. McCaffery, Mol. Phys. **35**, 617 (1978).

[3] S. R. Jeyes, A. J. McCaffery, and M. D. Rowe, Mol. Phys. **36**, 1865 (1978).

[4] H. Katô, S. R. Jeyes, A. J. McCaffery, and M. D. Rowe, Chem. Phys. Lett. **39**, 573 (1976).

[5] M. D. Rowe and A. J. McCaffery, Chem. Phys. **34**, 81 (1978).

[6] A. J. McCaffery, Spec. Per. Rep. **4**, 47 (1981).

[7] A. J. McCaffery, M. J. Proctor, and B. J. Whitaker, Annu. Rev. Phys. Chem. **37**, 223 (1986).

[8] P. A. Madden, Chem. Phys. Lett. **35**, 521 (1975) (note that a small error in Madden's formulas are corrected in Ref. 3).

[9] J. A. Guest, M. A. O'Halloran, and R. N. Zare, Chem. Phys. Lett. **103**, 261 (1984).

[10] M. Kroll J. Chem. Phys. **63**, 319, 1803 (1975).

[11] B. J. Whitaker and A. J. McCaffery, J. Chem. Phys. **78**, 3857 (1983).

[12] R. N. Dixon and D. Field, Proc. R. Soc. London, Ser. A. **366**, 247 (1982).

[13] A. J. Bain and A. J. McCaffery, J. Chem. Phys. **80**, 12 (1984).

[14] M. A. Auzinsh and R. N. Ferber, *Optical Polarization of Molecules* (Cambridge University Press, Cambridge, 1996).

[15] R. N. Zare, *Angular Momentum* (Wiley, New York, 1988).

[16] F. W. Birss, M. F. Merienne-Lafore, D. A. Ramsay, and M. Vervloet, J. Mol. Spectrosc. **85**, 493 (1981); C. G. Harkin, Ph.D. thesis, University of Sussex, 1987 (unpublished).

[17] S. Mayama, S. Hiraoka, and K. Obi, J. Chem. Phys. **80**, 7 (1984).

[18] Z. T. AlWahabi, C. G. Harkin, A. J. McCaffery, and B. J. Whitaker, J. Chem. Soc. Faraday Trans. II **85**, 1009 (1989).

[19] K. Blum, *Density Matrix Theory and Its Applications* (Plenum, New York, 1981).

[20] K. Dressler and D. A. Ramsay, Philos. Trans. R. Soc. London, Ser. A **251**, 553 (1959).

[21] C. Townes and A. W. Schawlow, *Microwave Spectroscopy* (Van Nostrand, Reinhold, New York, 1957).

[22] R. S. Lowe, J. V. V. Kasper, G. W. Hills, W. Dillenschneider, and R. F. Curl, Jr., J. Chem. Phys. **70**, 3356 (1979).